JOURNAL OF MATERIALS SCIENCE 30 (1995) 3924–3929

Solid-state amorphization behaviour in Ni/Zr multilayers with oxygen contamination

SUNG-MAN LEE, DONG-SIK YUN, IN-TAK NAM
Department of Materials Engineering, Kangwon National University, 192-1, Hyoja-Dong, Chunchon, KangWon-Do, Korea

JAI-YOUNG LEE, YONG-GYOO KIM, SANG-GWEON CHANG
Department of Materials Science and Engineering, Korea Advanced Institute of Science and Technology, Kusong Dong 373-1, Yusong Gu, Taejon, Korea

The solid-state amorphization by the interdiffusion reaction in sputter-deposited Ni–Zr multilayer films with oxygen contamination has been investigated by differential scanning calorimetry and X-ray diffractometry. Through X-ray photoelectron spectroscopy analysis, it was found that the multilayer films were contaminated with oxygen during deposition in a low-vacuum system (10^{-5} torr), and the concentration was modulated having the maximum in zirconium-rich regions. The kinetics of amorphization reactions has been examined by non-isothermal and isothermal annealing. Oxygen introduced into the sample during sample preparation and annealing treatments appears to affect the kinetics of the amorphization reaction associated with variation of the activation energy for interdiffusion in the amorphous layer and a critical thickness of the amorphous layer. The origins of abnormal behaviour in forming intermetallic compound as well as amorphous phase, are discussed in the context of the oxygen incorporation.

1. Introduction

It is well established experimentally that an amorphous alloy can be obtained by interdiffusion in thin-film diffusion couples consisting of elemental crystalline metals. The formation of such metastable amorphous phases is preferred over the stable crystalline state if the combination of the multilayers has a large negative heat of mixing which acts as a driving force for the reaction and if one of the elements of the multilayer shows an anomalously fast mobility. However, the formation of amorphous phase by solid-state diffusion has been found to be strongly influenced by annealing atmosphere during interdiffusion.

Hauser [1] investigated the effect of residual gases in amorphization of Ni–Zr multilayer films and showed that an amorphous phase was formed by annealing in a vacuum of $4–6 \times 10^{-7}$ torr (1 torr = 133.322 Pa) but annealing in ultrahigh vacuum conditions (10^{-12} torr) did not lead to amorphization. On the other hand, Van Rossum *et al.* [2] suggested that oxygen forms a diffusion barrier that inhibits the solid-state amorphization reaction. Most previous studies have been reported in systems that have in common an element having a strong affinity with oxygen. Indeed, one can expect oxygen contamination during both annealing treatment and multilayer sample preparation. However, the effect of impurities incorporated during deposition on the amorphization reaction has not been investigated previously. It should also be noted that, in most previous studies, multilayer diffusion couples were prepared in an ultrahigh vacuum system (higher than 5×10^{-8} torr) [3–5].

In this paper, we report the results of solid-state amorphization on Ni–Zr multilayer films deposited in a low-vacuum system (base pressure 10^{-5} torr). Differential scanning calorimetry (DSC) was utilized to monitor the progress of the solid-state amorphization reaction. The structures and phases of the samples in the as-prepared state, as well as at various degrees of reaction, were characterized by X-ray diffractometry (XRD). These techniques have been successfully used to study the amorphization of thin multilayered films by diffusion reaction in the solid state [4–7].

2. Experimental procedure

Ni–Zr multilayer films were prepared by magnetron sputter deposition with a base pressure of 10^{-5} torr. The substrates were rotated during deposition to ensure the uniformity of the sample. The substrate temperature was kept at about 323 K. The prepared multilayer films have an average composition of $Ni_{50}Zr_{50}$ and $Ni_{64}Zr_{36}$, and a modulation wavelength of 55 nm. The deposition rates and resulting film thicknesses were calibrated using an Alpha step 2000 thickness meter.

Thermal analysis was performed using a differential scanning calorimetry (Perkin–Elmer DSC7) with argon purified through the moisture and oxygen traps as the purge gas. Samples to be used for calorimetric

0022–2461

analysis were deposited on NaCl substrates (produced as a window of an infrared spectrometer). After deposition, the multilayer films were removed from their substrates by dipping the samples in deionized water.

The composition profiles of the as-deposited $Ni_{64}Zr_{36}$ film were analysed using X-ray photoelectron spectroscopy (VG Scientific ESCALAB 200/R).

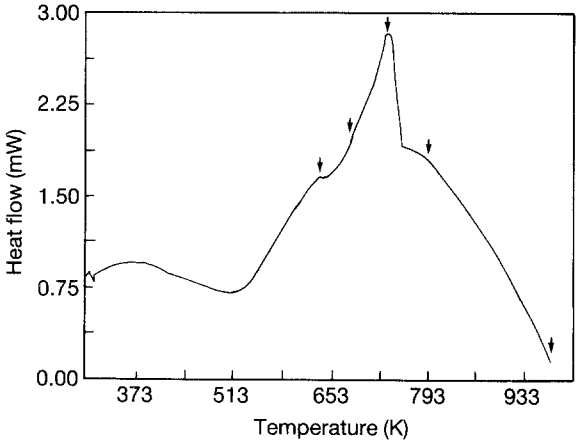

Figure 1 Differential scanning calorimetry trace obtained on heating an $Ni_{50}Zr_{50}$ multilayer at 10 K min^{-1}. (↓ = XRD results of b–f in fig. 2).

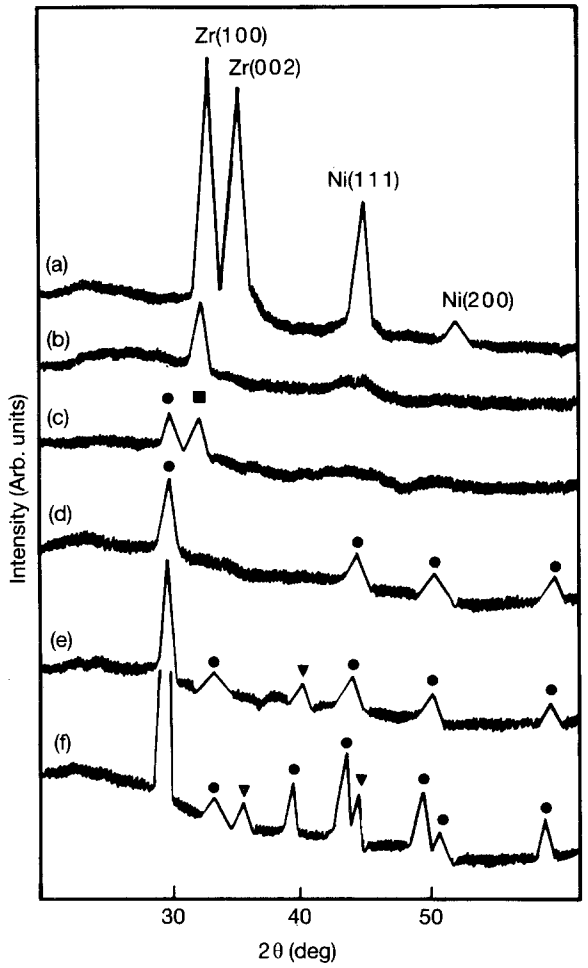

Figure 2 X-ray diffraction profiles for $Ni_{50}Zr_{50}$ multilayer films which had been heated from 303 K to various temperatures at a rate of 10 K min^{-1} and cooled rapidly to room temperature in the differential scanning calorimeter: (a) as-deposited, (b) after heating to 633 K, (c) after heating to 673 K, (d) after heating to 733 K, (e) after heating to 783 K, (d) after heating to 968 K. (●) Ni_7Zr_2, (■) Zr, (▼) $NiZr_2$.

Isothermal anneals for the samples deposited on to glass substrates (Corning 7059 glass) were performed in a vacuum of 10^{-5} torr.

3. Results and discussion

The DSC trace of multilayer samples with overall composition $Ni_{50}Zr_{50}$ is shown in Fig. 1, and it reveals some features of solid-state reactions in the Ni–Zr system. The broad exothermic DSC signal observed below 633 K is associated with the amorphization process, in which nickel is almost consumed (Fig. 2b). It is remarkable that an endothermic reaction peak is found during a DSC scan of Ni–Zr multilayer thin films. An X-ray diffraction profile of a sample heated to 673 K and quenched to room temperature reveals that crystalline compound Ni_7Zr_2 begins to be formed at the early stage of the endothermic reaction in the DSC scan. The final crystallization products consist of Ni_7Zr_2 and $NiZr_2$ intermetallic compounds.

The DSC scan of Ni/Zr multilayers of average stoichiometry $Ni_{64}Zr_{36}$ is shown in Fig. 3, and it is similar to that of the $Ni_{50}Zr_{50}$ system shown in Fig. 1. This scan was conducted at a constant scan rate of 10 K min^{-1}. It is observed that two exothermic and one endothermic peaks appear. Note that an endothermic peak is also found in this sample.

Fig. 4 shows the X-ray diffraction patterns of samples heated at 10 K min^{-1} in the DSC to various temperatures indicated with arrows in Fig. 3 and then quenched to room temperature. Peaks corresponding to crystalline nickel and zirconium are present in the as-deposited sample (Fig. 4a). From the peak positions, the values of the lattice constants determined for zirconium and nickel are larger than those known from the literature. For example, the zirconium lattice is expanded about 2%. For the sample heated to 593 K, the intensities of the crystalline zirconium and nickel peaks significantly decrease. After 673 K (i.e. after the endothermic peak in Fig. 3), the intensity of the crystalline zirconium peak is nearly lost. The decline in intensity with heating temperature of the

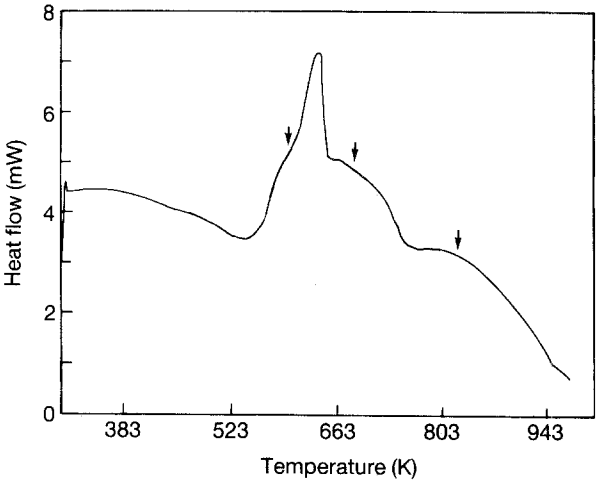

Figure 3 Differential scanning calorimetry (DSC) trace for an Ni–Zr multilayer film of average stoichiometry $Ni_{64}Zr_{36}$ and a modulation wavelength of 55 nm. The heating rate was 10 K min^{-1}. (↓ = XRD results of b–d in fig. 2).

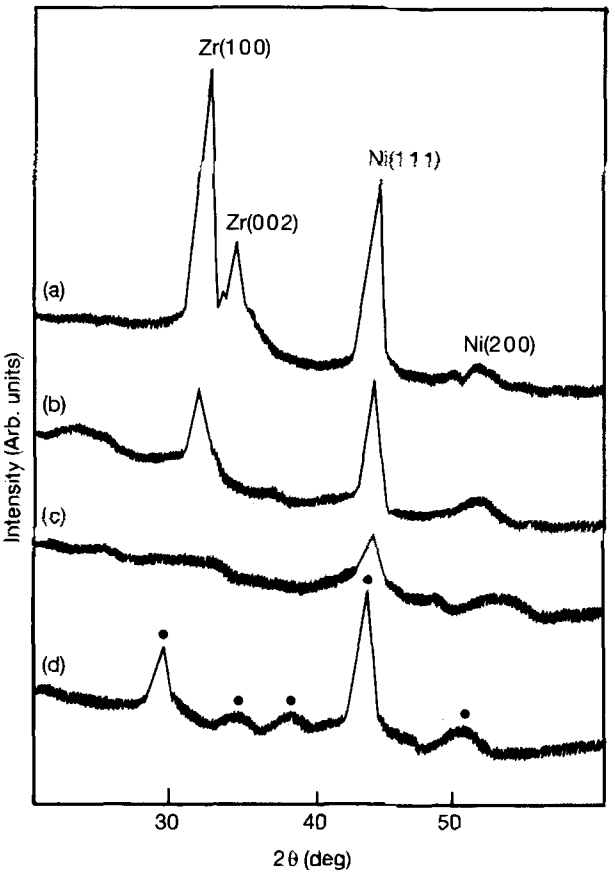

Figure 4 X-ray diffraction profiles for Ni/Zr multilayer films which had been heated from 303 K to various temperatures at a rate of 10 K min^{-1} and cooled rapidly to room temperature in the differential scanning calorimeter: (a) as-deposited, (b) after heating to 593 K, (c) after heating to 673 K, (d) after heating to 813 K. (●) Ni_7Zr_2.

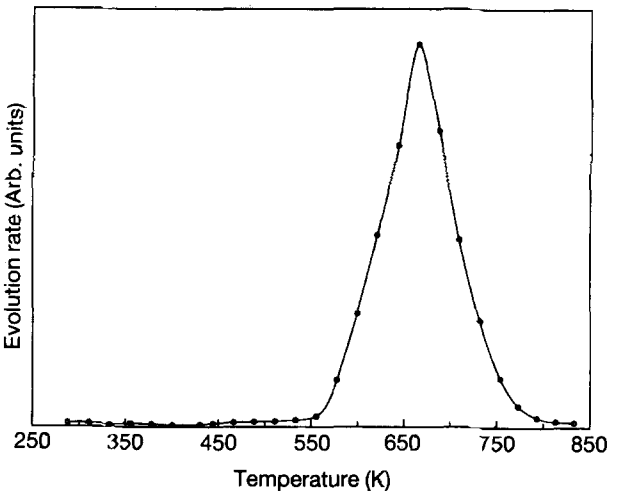

Figure 5 The gas desorption curve for an Ni–Zr multilayer film of average stoichiometry $Ni_{64}Zr_{36}$ heated at 4 K min^{-1}.

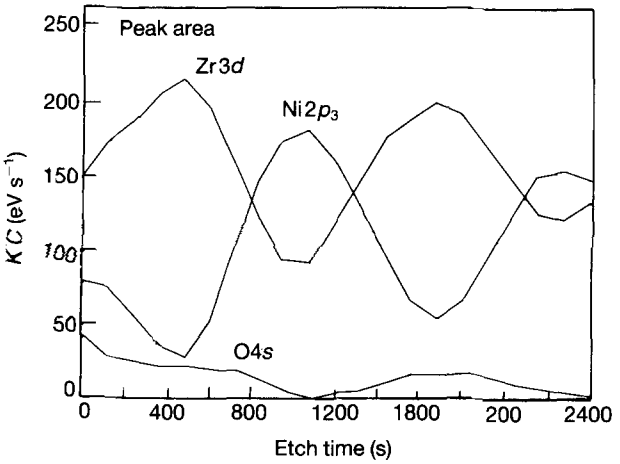

Figure 6 XPS depth profile of $Ni_{64}Zr_{36}$ multilayer thin film.

crystalline zirconium and nickel reflections provides a measure of the consumption of these elemental components. From the absence of Bragg peaks that can be associated with crystalline phase formation, we infer a corresponding growth of amorphous Ni–Zr. Therefore, although the traces shown in Fig. 4 are not normalized to the same incident X-ray intensity, a qualitative conclusion is possible: the solid-state reaction in the temperature range up to 673 K is associated with the formation of an amorphous phase. However, as the amorphization of an elemental Ni–Zr diffusion couple is known to be characterized by exothermic reaction in DSC scans, the endothermic peak shown in Fig. 3 must to be ascribed to a reaction other than amorphization.

Fig. 5 shows the gas thermal desorption curve for a similar sample at a heating rate of 4 K min^{-1} using a gas thermal desorption technique by means of the gas chromatography [8], and the evolved gas is confirmed to be oxygen. Only one peak appears in the gas evolution spectra and the position of this corresponds to the endothermic peak temperature shown in Fig. 3. The Ni–Zr multilayers as-deposited having an average composition of $Ni_{64}Zr_{36}$ were investigated by X-ray photoelectron spectroscopy (XPS), and it is confirmed that the prepared films are contaminated with oxygen, in which the maximum of oxygen occurs in zirconium-rich regions, as shown in Fig. 6. The valence band spectrum of the zirconium layer is in good agreement with that of pure zirconium, indicating that a Zr–O complex or oxide is not formed as a result of oxygen incorporation. It was also found that the endothermic peak position is dependent on the overall composition of multilayer samples (e.g. for the $Ni_{50}Zr_{50}$ sample, centred at 733 K as shown in Fig. 1) but not on the wavelength of the multilayer. In addition, in the DSC scan for a monolayer of zirconium, the endothermic peak appears at 803 K at a heating rate of 10 K min^{-1}. These results indicate that the endothermic reactions observed in DSC scans (Figs 1 and 3) are associated with the evolution of oxygen from the amorphous phase formed earlier in the low-temperature range.

In case of the $Ni_{50}Zr_{50}$ sample, the nickel layers have been completely dissolved while there is still elemental zirconium present, as shown in Fig. 2. To react the residual zirconium, it is necessary for the nickel atoms to diffuse out of the amorphous NiZr into the elemental zirconium layers. However, this reaction seems to be rather difficult because oxygen introduced into zirconium is immobile in the temperature range mentioned above. That the compound

Ni_7Zr_2 forms first in this solid-state reaction seems to be abnormal in view of the composition of the amorphous material at the interface between the growing amorphous phase and the crystalline zirconium [9]. Previous study has shown that the intermetallic NiZr phase starts to form at the zirconium interface, provided there is still unreacted zirconium present [7, 10].

The observed discrepancies may probably be explained in the following way. The solid-state amorphization reaction is achieved by motion of one constituent only, while the movement of both constituents is required to form a crystalline compound. Nickel is known to be the dominant species in the amorphization in Ni/Zr diffusion couples [11, 12]. The suppression of the NiZr formation indicates that a barrier to zirconium diffusion has formed. Oxygen introduced into the zirconium layer is unlikely to diffuse into the growing crystalline compound layer because oxygen and zirconium are strongly bonded and the diffusivity of an Zr–O complex should be very low. Oxygen thus accumulates near the Zr/Ni–Zr compound interfaces as zirconium leaves to diffuse into the growing compound layer. In addition, oxygen in zirconium may form zirconium oxide at the crystalline compound–zirconium interface, which may play a role as a barrier to zirconium diffusion. Therefore, the supply of zirconium atoms is not sufficient to allow the NiZr compound to form, but may allow Ni_7Zr_2 to form, thus altering the first phase formed.

In metal–metal diffusion couples, a metastable amorphous phase may form initially and grow to substantial thickness prior to the onset of the formation of crystalline compound, i.e. a critical thickness [13]. The X-ray diffraction data of Fig. 4 indicate that Ni_7Zr_2 is the first intermetallic compound to form. This is not in accord with the nominal overall composition of the as-deposited multilayer $Ni_{64}Zr_{36}$. Furthermore, the residual reflection of nickel is still observed for the sample heated up to the temperature at which the DSC peak corresponding to the formation of Ni_7Zr_2 begins. This is viewed as evidence that upon heating of the Ni/Zr multilayer at 10 K min^{-1}, complete amorphization has not been accomplished. Because the modulation wavelength of the multilayer used in this study is 55 nm, it seems that the critical thickness of the amorphous layer is smaller than that of 100 nm previously observed in the Ni–Zr system [3, 4].

The constant heating rate DSC scans using multilayer thin films enable the growth kinetics of amorphization to be investigated quantitatively. To a good approximation, the activation energy for interdiffusion in the amorphous layer during the solid-state amorphization reaction can be determined from a DSC scan using, for example, Equation 1 [4–6]

$$\ln(H\mathrm{d}H/\mathrm{d}t) = E/kT + \text{constant} \qquad (1)$$

where H is the area of the amorphization peak on a DSC trace integrated from the onset of reaction to temperature T, $\mathrm{d}H/\mathrm{d}t$ is the heat flow in the DSC at temperature T and k is the Boltzmann constant.

From Equation 1, a plot of $\ln(H\mathrm{d}H/\mathrm{d}t)$ against $1/T$ will give a straight line whose gradient enables the activation energy for interdiffusion in the amorphous alloy to be found as shown in Fig. 7. In Fig. 7, the two curves, which are derived from DSC traces obtained by heating similar multilayer $Ni_{64}Zr_{36}$ at different heating rates of 10 and 5 K min^{-1}, have essentially the same gradient. The points represented by stars are derived from the DSC trace shown in Fig. 3. The deviations of the experimental curves from a straight line in Fig. 7 have also been previously observed by other workers [5], who have suggested that the departure of the curves from a straight line at the high-temperature end is associated with a consequence of the supply of one or both elements being exhausted. However, the X-ray diffraction pattern shown in Fig. 4b shows that crystalline elements, zirconium and nickel, still remain even at 593 K, which is higher than 523 K where the deviation of the curve from a straight line begins. Therefore, such a departure shown in Fig. 7 is ascribed to a sudden decrease in the reaction rate caused by a decrease of atomic mobility during amorphization rather than the supply of one or both elements being exhausted.

The slope of the best straight line drawn in Fig. 7 yields an activation energy of 0.6 ± 0.05 eV, which is smaller than 1.1 eV obtained by other workers [3, 4]. It should be noted that base pressures were less than 10^{-8} torr in previous studies, while it was 10^{-5} torr in this study. In this respect, the low value of activation energy seems to be attributed to oxygen incorporated during the sample preparation in a low-vacuum system, which assists the solid-state amorphization reaction in multilayer Ni–Zr.

Based on the small values of the critical thickness of the amorphous layer and activation energy, the effect of oxygen on the solid-state amorphization reaction can be explained as follows. First, the low value of activation energy suggests that the oxygen promotes

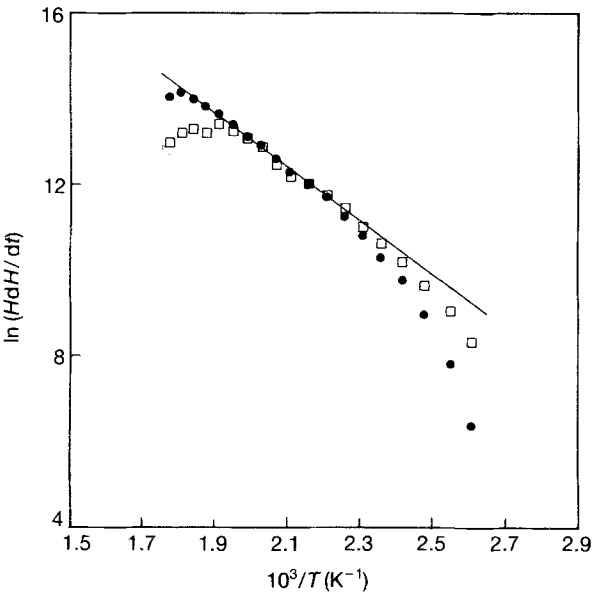

Figure 7 Plots of $\ln(H\mathrm{d}H/\mathrm{d}t)$ versus the reciprocal of absolute temperature for the DSC traces of the $Ni_{64}Zr_{36}$ sample obtained by heating at (●) 10 K min^{-1} and (□) 5 K min^{-1}.

the interdiffusion for the formation of an amorphous interlayer. It has been previously reported that oxygen may promote the interdiffusion and/or reaction [1, 14, 15]. On the other hand, the mobility of atomic diffusion during growth of the amorphous interlayer is considered to play an important role in determining its maximum thickness. As the amorphous phase becomes thicker, the oxygen will be incorporated in the growing amorphous Ni–Zr layer and occupy the interstices in the amorphous phase. In addition, because nickel atoms in amorphous material Ni–Zr diffuse by an interstitial-like mechanism [16], the sites occupied by oxygen are no longer available for the diffuser, and the long-range migration of the diffuser is retarded by the presence of oxygen. Alternatively, oxygen accumulates near the interfaces of amorphous phase/Zr and amorphous phase/Ni, thus the interdiffusion can be hindered by the oxygen atoms at the interfaces. The hindrance of diffusion favouring the amorphization reaction may result in the production of a thermodynamically stable intermetallic compound. Although the oxygen atoms incorporated in the amorphous interlayer evolve upon further heating, as evinced by the endothermic peak in the DSC trace (as shown in Fig. 3), thereafter the reaction temperature is so high that the growth of the amorphous phase is not favoured compared to the competing growth of the crystalline equilibrium phases (intermetallic compounds). The progress of the amorphization reaction in multilayer thin films during isothermal annealing can be monitored with the X-ray peak intensity change, from the viewpoint that the amounts of crystalline phases remaining after a certain time, t, are proportional to the integrated intensities of the crystal

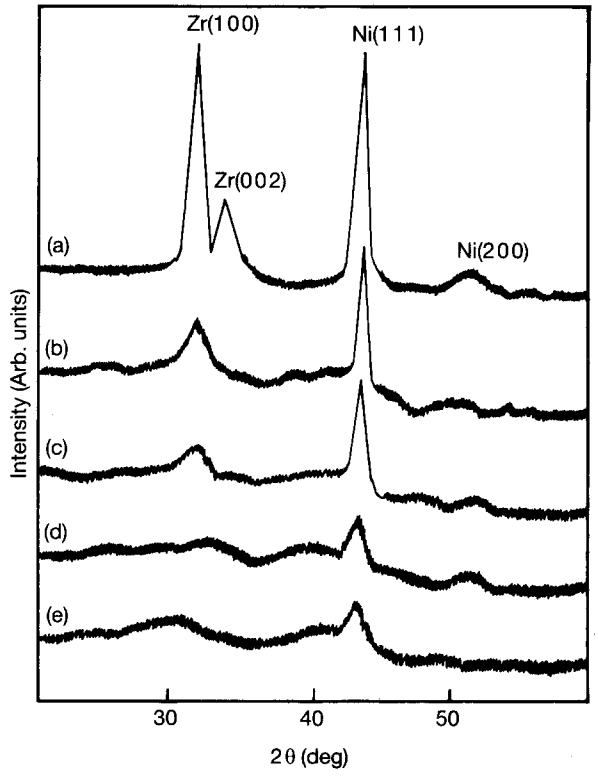

Figure 8 X-ray diffraction pattern of the $Ni_{64}Zr_{36}$ sample for several annealing times at 553 K: (a) as-deposited, (b) 1 h, (c) 1.4 h, (d) 2 h, (e) 2.5 h. The intensity (300 counts full scale) is the same for each pattern.

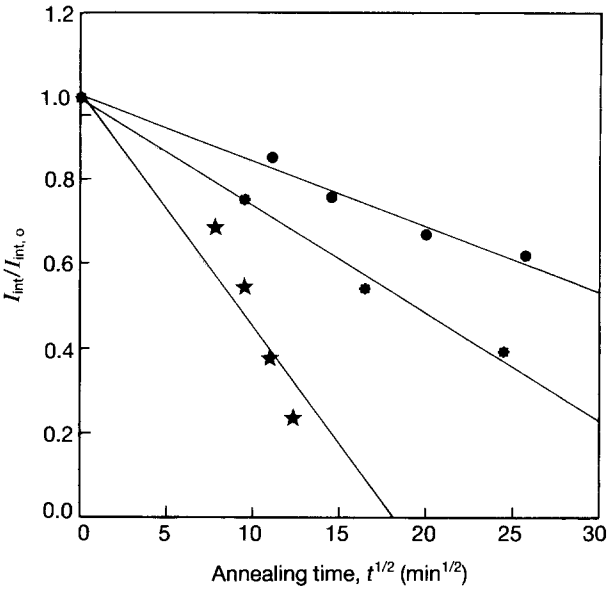

Figure 9 Relative integrated intensity, $I_{int}/I_{int,0}$ for Ni(1 1 1) as a function of annealing time at a given annealing temperature: (●) 513 K, (✱) 533 K, (★) 553 K.

reflections. Fig. 8 shows XRD profiles for the multilayer $Ni_{64}Zr_{36}$ sample with the progressive annealing time at 553 K. As expected, the integrated intensities of the Ni{1 1 1} and Zr{1 0 0} and {0 0 2} reflections decrease with time. The XRD patterns do not reveal any sign of intermediate crystalline phases, but indicate amorphous phase formation during the solid-state reaction.

The quantity of remaining nickel is estimated from the integrated intensities of the Bragg peak on each pattern, and the relative integrated intensity, $I_{int}/I_{int,0}$, is plotted as a function of the square root of the annealing time in Fig. 9. It can be noted that there is evidence of a parabolic time law for the reaction times used. This probably implies a diffusion-limited growth of the amorphous layer. The kinetics information for amorphization can be deduced by using the cross-cut method [17] for isothermal annealing experiments shown in Fig. 9. The activation energy, E, is immediately calculable from

$$\ln(t_1/t_2) = (1/T_1 - 1/T_2)E/k \qquad (2)$$

where t_1 and t_2 are the time required to reach a constant value of reacted material at temperature T_1 and T_2. This method gives an average activation energy of 1.24 ± 0.5 eV, which is twice as large as the previous one measured during isochronal DSC scans. It should be remarked that, while an inert-gas atmosphere (argon) purified through oxygen and moisture traps was used for isochronal DSC annealing, the isothermal annealing took place in a vacuum of 10^{-5} torr. The concentration of oxygen was found to increase after annealing Ni–Zr layers in a rough vacuum [14]. Therefore, the Ni–Zr multilayers could be more contaminated with oxygen during isothermal annealing than in the case of the DSC annealing. In this context, it is presumed that the highly differing results for the amorphization reaction kinetics show the concentration dependence of the effect of oxygen on the solid-state amorphization reaction.

4. Conclusion

The solid-state interdiffusion reactions in Ni–Zr multilayer films with contamination have been investigated by means of differential scanning calorimetry and X-ray diffraction. The endothermic peak was observed in a DSC scan of an as-deposited sample, which is associated with the evolution of oxygen from the amorphous phase formed earlier at low temperatures. The kinetics of the amorphization reactions examined by differential scanning calorimetry appears to indicate that oxygen incorporated during sample preparation by the sputtering technique under a low-vacuum system (base pressure 10^{-5} torr) leads to a lower activation energy for interdiffusion and a smaller critical thickness of the amorphous layer compared with previously reported values. However, the isothermal analysis performed in a vacuum of 10^{-5} torr, in which the possibility of oxygen contamination can be raised, gives an activation energy twice as large as the previous one. It is presumed that the effect of oxygen on the amorphization reaction kinetics is dependent on the oxygen content. The abnormal behaviour in forming intermetallic compound phases and amorphous phase as a result of oxygen incorporation is discussed.

Acknowledgement

This work was financially supported by the Korea Science and Engineering Foundation through contact 901-0602-014-2.

References

1. J. J. HAUSER, *Phys. Rev. B* **32** (1985) 2887.
2. M. VAN ROSSUM, M. A. NICOLT and W. L. JOHNSON, *ibid.* **29** (1984) 5498.
3. S. B. NEWCOMB and K. N. TU, *Appl. Phys. Lett.* **48** (1986) 1436.
4. E. J. COTTS, W. J. MENG and W. L. JOHNSON, *Phys. Rev. Lett.* **57** (1986) 2295.
5. R. J. HIGHMORE, J. E. EVETTS, A. L. GREER and R. E. SOMEKH, *Appl. Phys. Lett.* **50** (1987) 566.
6. B. E. WHITE Jr, M. E. PATT and E. J. COTTS, *J. Appl. Phys.* **68** (1990) 1910.
7. G. C. WONG, W. L. JOHNSON and E. J. COTTS, *J. Mater. Res.* **5** (1990) 488.
8. H. G. LEE and J. Y. LEE, *Acta Metall.* **32** (1984) 131.
9. J. C. BARBOUR, *Phys. Rev. Lett.* **55** (1985) 2872.
10. J. ECKERT, L. SCHULTZ and K. URBAN, *J. Mater. Res.* **6** (1991) 1874.
11. Y. T. CHENG, W. L. JOHNSON and M. A. NICOLET, *Appl. Phys. Lett.* **47** (1985) 800.
12. H. HAHN and R. S. AVERBACK, *Phys. Rev. B* **37** (1988) 6537.
13. W. L. JOHNSON, *Prog. Mater. Sci.* **30** (1986) 81.
14. B. M. CLEMENS, *Bull. Am. Phys. Soc.* **29** (1984) 506.
15. M. KITADA, N. SHIMIZU and H. TANABE, *J. Mater. Sci.* **26** (1991) 835.
16. H.-M. WU, H. HAHN and R. S. AVERBACK, *Mater. Res. Soc. Symp. Proc.* **187** (1990) 27.
17. W. E. PARKINS, G. J. DIENES and F. W. BROWN, *J. Appl. Phys.* **22** (1951) 1012.

Received 19 February 1993
and accepted 7 June 1994